

**THE MANEV TWO-BODY PROBLEM:  
QUANTITATIVE AND QUALITATIVE THEORY**

**FLORIN N. DIACU, VASILE MIOC, CRISTINA STOICA**

**DMS-686-IR**

**October 1994**

# THE MANEV TWO-BODY PROBLEM: QUANTITATIVE AND QUALITATIVE THEORY.

Florin N. DIACU\*

*Department of Mathematics and Statistics  
University of Victoria, P.O. Box 3045  
Victoria, British Columbia, CANADA, V8W 3P4  
Phone: (604)721-6330, Fax: (604)721-8962  
e-mail: diacu@sol.uvic.ca*

Vasile MIOC

*Astronomical Institute of the Romanian Academy  
Astronomical Observatory Cluj-Napoca  
Str. Cireşilor 19, 3400 Cluj-Napoca, ROMANIA*

Cristina STOICA

*Institute for Gravitation and Space Science  
Bd. Ana Ipătescu 21, 71111 Bucharest, ROMANIA*

---

\* Supported in part by NSERC grant 3-48376

### Abstract

Manev's gravitational law, given by a potential function of the form  $U(r) = \nu/\rho + \mu/\rho^2$ , where  $\rho$  is the distance between particles and  $\nu, \mu$  are positive constants, is a good substitute of relativity within the frame of classical mechanics. We first obtain exact formulas of the trajectory and of the nodal period in the two-body problem. Then we proceed to a qualitative study of this problem near collision and describe the geometry of the phase space. We show that a *black hole* effect is characteristic to this model. This implies that the set of collisions has positive measure and that collisions are not regularizable.

## 1. Introduction

The mathematical study of Manev's gravitational model (or Maneff—in German and French spelling) has been recently initiated by two studies on the qualitative behavior of particles near collisions [1], [2]. In [1] an anisotropic model has been also proposed in order to understand the possible connections between classical and quantum mechanics. Such studies are fully justified from the physical point of view since, at the level of the solar system at least, Manev's law provides the same good theoretical approximations offered by general relativity (see [5]). Today's methods of experimental physics show that if considering the corresponding field equations, theory and practice match very well together. Our point of view is to offer a projection of the field equations in a classical mechanics framework in order to satisfy the needs of celestial mechanics.

General relativity was able to answer many important questions in physics and astronomy. Unfortunately, all the attempts to formulate a meaningful relativistic  $n$ -body problem have failed to provide valuable results. Therefore, already in the twenties, there has occurred the necessity to create a model that could respond to the theoretical needs of celestial mechanics. Prerelativistic attempts had been rather unsuccessful in this sense.

It is not easy to find a suitable model, within classical mechanics, which maintains the advantages of the Newtonian one and also makes the necessary corrections such that orbits coming close to collisions match theory with observation. The many pre- and post-relativistic attempts to obtain such models have usually managed to answer certain question (as those regarding the perihelion advances of the inner planets) but failed to explain other phenomena (as the motion of the moon); see [5]. There has been one exception, a law given by a potential of the type  $\nu/\rho + \mu/\rho^2$ , where  $\rho$  is the distance between two particles and  $\nu, \mu$  are positive, suitably chosen, constants. This has been used by Einstein himself as an approximation of relativity in order to compute the correct perihelion advance of Mercury; it has also been proposed by Manev, [6], [7], [8], [9] (in the twenties, in a form close to the one we are using here) as an alternative classical substitute of relativity.

But Manev was not the first one to think of it. Two and a half centuries before him, Isaac Newton himself considered this model. He didn't feel happy enough with his (today) classical model, and studied the same potential  $\nu/\rho + \mu/\rho^2$  for more than twenty years after the publication of *Principia*. The reason behind Newton's frustration with the inverse square force law was his impossibility to explain the apsidal motion of the moon. Most of Newton's research on the Manev-type model remained unpublished during his life-time, appearing only around 1850 in his—today famous—Portsmouth Collection of manuscripts. There was one exception. A result published in *Principia* (Book I, Article IX, Theorem IV, Corollary 2), showed that in the frame of this exotic model, the motion in a center-force problem is not an ellipse, but a *precessional ellipse*, i.e. one that rotates in its own plane of motion. This is in fact the true motion of Mercury which cannot find a good explanation (within the classical Newtonian model) with the help of perturbation theory.

Clairaut later reconsidered Newton's Manev-type model feeling the same frustration in the impossibility to explain the motion of the moon. Later, however, he found an argument within the framework of the classical Newtonian model and gave up his endeavors on the

Manev-type law.

Poincaré himself questioned the validity of the Newtonian model, when, in a popular account on the stability of the solar system, [17], published in 1898, he wrote: “One of the questions with which researchers have been most preoccupied is that of the stability of the solar system. This is, if truth be told, more a mathematical question than a physical one. Even if one were to discover a general and rigorous proof, one could not conclude that the solar system is eternal. It may, in fact, be subject to forces other than those of Newton.” This came at a time when the world of physics was already searching a new path, a search that would eventually lead towards the discovery of quantum mechanics and relativity.

The goal of this paper is to provide the basics for future studies of Manev’s model by presenting the main quantitative and qualitative results of the two-body problem. Some of them are already known but are hard to find in the literature. Besides, we thought that they deserve a systematic treatment. Moreover, the modern geometrical setting we provide and the new methodology we apply in the second part of our paper (which provides a qualitative study of the problem) allows a better understanding of the phenomena encountered near collision.

Sections 2,3, and 4 are dealing with quantitative methods, while Sections 5 and 6 are treating qualitative aspects. In Section 2 we describe the basic equations used for our quantitative endeavors. We consider the Newton-Euler equations which help us later in Section 3 to obtain the exact solution of the two-body problem with the help of perturbation methods. We give a full description of the orbit behavior, generalizing the early result published in Newton’s *Principia*. We devote Section 4 to a rather astronomical aspect of the problem and show that the nodal period can be explicitly computed. This will close the quantitative results of this paper.

The qualitative part starts with Section 5 where we introduce McGehee-type transformations, [10]. This is a modern technique, which allows a better understanding of the motion of particles in the neighborhood of collisions. We obtain equivalent, *regularized* equations of motion, i.e. equations free of singularities. The singularities have been blown up providing instead a so-called *collision manifold*, which, in our case, is given by a 2-dimensional torus in a 3-dimensional phase space. The torus is thus naturally pasted to the phase space and the flow can be extended to the torus. Though having no direct correspondence in the physical reality, the flow on the torus offers information on the behavior of the particles near the collision. Every orbit tending to the torus is a collision solution and every orbit leaving the torus represents an ejection solution. In Section 6 we perform a qualitative study of the flow on and near the collision manifold (see Figures 1,2, and 3). We show that the flow on the torus is formed by periodic orbits with the exception of the upper and lower circles which are filled with fixed points. The phase space is foliated by cylinders having as common axis the line perpendicular to the planes of the periodic orbits of the torus and which passes through their centers. From each fixed point of the upper circle ejects one single orbit (Figure 2) and each fixed point of the lower circle is finally hit by one single orbit. These correspond to the motion of particles colliding such that their individual orbits have asymptotically a common tangent. Also, from each periodic orbit of the upper part of the torus ejects a manifold of solutions (Figure 3). They all lie on the cylinder perpendicular on the plane of the circle. Symmetrically, a manifold of orbits will

tend to each periodic orbit belonging to the lower part of the torus. All these are orbits of small angular momentum which lead to collisions after one of the particles is rotating infinitely many times around the other particle: a *black hole effect*. These prove that the set of initial data leading to collisions has positive measure, therefore the probability of collision is a positive number. A further study of the flow shows that the solutions are not *block-regularizable*, (see [3]), i.e. there is no meaningful continuation of the orbit beyond the collision, on the same energy level.

## 2. Basic Equations

Consider two particles of positive masses  $m_1$  and  $m_2$  moving in the Euclidean space under the influence of Manev's gravitational law. Their coordinates, in a fixed frame, are given by the vectors  $\mathbf{q}_1$  and  $\mathbf{q}_2$ . The equations of motion read

$$\ddot{\mathbf{q}} = -(\mu/\rho^3)\mathbf{q} - [3\mu^2/(c^2\rho^4)]\mathbf{q}, \quad (2.1)$$

where  $\mathbf{q} = (\mathbf{q}_1, \mathbf{q}_2)$  is the *configuration* of the system,  $\rho = |\mathbf{q}|$  represents the Euclidean distance between  $m_1$  and  $m_2$ ,  $\mu = G(m_1 + m_2)$  is the *gravitational parameter*,  $G$  denotes the gravitational constant, and  $c$  is the speed of light.

Standard results of the differential equations theory ensure that for initial conditions  $(\mathbf{q}, \dot{\mathbf{q}})(t_0)$ , with  $\mathbf{q} \neq 0$ , the equations (2.1) have a unique solution defined on a maximal interval containing  $t_0$ . As we will see in Section 5, this maximal interval is the whole real axis except for the cases when the motion leads to a collision.

On the extent of our quantitative endeavors we will regard the equations (2.1) as the classical Newtonian ones with a correction term. This will enable us to apply the methods of perturbation theory by considering the deviations of the trajectory from a Keplerian one as mere perturbations.

Let us consider further the Newton-Euler equations (see e.g. [19], [15]) which describe the motion of  $m_2$  relative to a frame having the origin at  $m_1$ , in terms of the following Keplerian osculating elements:

- $a$  = semimajor axis,
- $\Omega$  = longitude of ascending node,
- $i$  = the inclination of the orbit plane,
- $e$  = eccentricity,
- $\omega$  = argument of pericenter,
- $u$  = argument of latitude.

We will also use the *semilatus rectum*  $p = a(1 - e^2)$ , the *true anomaly*  $v = u - \omega$ , and the parameters  $q = e \cos \omega$  and  $k = e \sin \omega$  which are useful in studying orbits of small eccentricity. Notice that for  $i = 0$  the line of nodes (involved in defining  $\Omega, \omega$ , and  $u$ ) is undefined. In this case, since—as in the Newtonian model—the orbit is planar,  $\Omega, \omega$ , and  $u$  are defined with respect to a fixed (arbitrarily chosen) direction in the plane of the orbit.

The Newton-Euler equations take the form

$$\begin{cases} p' &= 2(Z/\mu)\rho^3 T \\ \Omega' &= (Z/\mu)\rho^3 W \frac{\sin u}{p \sin i} \\ i' &= (Z/\mu)\rho^3 W \frac{\cos u}{p} \\ q' &= (Z/\mu)\{\rho^3 k W \sin u \frac{\cot i}{p} + \rho^2 T[\rho \frac{(q+\cos u)}{p} + \cos u] + \rho^2 S \sin u\} \\ k' &= (Z/\mu)\{-\rho^3 q W \sin u \frac{\cot i}{p} + \rho^2 T[\rho \frac{(k+\sin u)}{p} + \sin u] - \rho^2 S \cos u\} \\ t' &= Z\rho^2 \sqrt{\mu p}, \end{cases} \quad (2.2)$$

where  $' = \frac{d}{du}$ ,  $Z = (1 - \rho^2 \Omega' \frac{\cos i}{\sqrt{\mu p}})^{-1}$ , and  $S, T, W$  are the classical radial, transversal, and binormal components, of the perturbing acceleration.

Since the perturbing force introduced by Manev is radial, the components of the perturbing acceleration are:  $S = -3\mu^2/(c^2 \rho^3)$ ,  $T = W = 0$ , and the equations (2.2) become

$$\begin{cases} p' = \Omega' = i' = 0, \\ q' = -[3\mu^2/(c^2 \rho)] \sin u \\ k' = [3\mu^2/(c^2 \rho)] \cos u \\ t' = \rho^2/\sqrt{\mu p}. \end{cases} \quad (2.3)$$

Newton-Euler systems are usually tackled in astronomy by successive approximations (see e.g. [14]) or by averaging-type techniques. In our case, however, the equations (2.3) can be solved explicitly. This will be done in the next section.

### 3. Orbit Behavior

If we attach to the equations (2.3) the initial conditions at  $u_0$ ,

$$(p, \Omega, i, q, k, t)(u_0) = (p_0, \Omega_0, i_0, q_0, k_0, t_0),$$

the first three equations in (2.3) yield

$$p \equiv p_0, \quad \Omega \equiv \Omega_0, \quad i \equiv i_0,$$

which also recovers the fact that each orbit is planar.

Applying now the methods of perturbation theory we introduce the expression of  $\rho$  from the orbit equation

$$\rho = p/(1 + e \cos v) = p/(1 + q \cos u + k \sin u)$$

into the equations (2.3) and obtain

$$\begin{cases} q' = -x \sin u (1 + q \cos u + k \sin u) \\ k' = x \cos u (1 + q \cos u + k \sin u), \end{cases} \quad (3.1)$$

where  $x = 3\mu/(c^2 p_0)$  is a small parameter. Its size is easy to estimate. For example, the Schwarzschild radius of the earth ( $R_{Sch} = 2\mu/c^2$ ) is equal to 1 cm, while a satellite orbit has  $p_0 > 6500$  km. This leads to a corresponding  $x$  of the order  $10^{-9}$  or smaller.

Solving the initial value problem attached to the equations (3.1), the solution reads:

$$\begin{aligned}
q(u) = & \left\{ \frac{1}{\sqrt{1-x}} \sin(\sqrt{1-x}(u-u_0)) [\sin(u-u_0) - x \cos u_0 \sin u] \right. \\
& \left. + \cos(\sqrt{1-x}(u-u_0)) \cos(u-u_0) \right\} q_0 \\
& + \left\{ \frac{1}{\sqrt{1-x}} \sin(\sqrt{1-x}(u-u_0)) [\cos(u-u_0) - x \sin u_0 \sin u] \right. \\
& \left. - \cos(\sqrt{1-x}(u-u_0)) \sin(u-u_0) \right\} k_0 \\
& + \frac{x}{1-x} [1 - \cos(\sqrt{1-x}(u-u_0))] \cos u \\
& - \frac{x}{\sqrt{1-x}} \sin(\sqrt{1-x}(u-u_0)) \sin u, \\
k(u) = & \left\{ -\frac{1}{\sqrt{1-x}} \sin(\sqrt{1-x}(u-u_0)) [\cos(u-u_0) - x \cos u_0 \cos u] \right. \\
& \left. + \cos(\sqrt{1-x}(u-u_0)) \sin(u-u_0) \right\} q_0 \\
& + \left\{ \frac{1}{\sqrt{1-x}} \sin(\sqrt{1-x}(u-u_0)) [\sin(u-u_0) + x \sin u_0 \cos u] \right. \\
& \left. + \cos(\sqrt{1-x}(u-u_0)) \cos(u-u_0) \right\} k_0 \\
& + \frac{x}{1-x} [1 - \cos(\sqrt{1-x}(u-u_0))] \sin u \\
& + \frac{x}{\sqrt{1-x}} \sin(\sqrt{1-x}(u-u_0)) \cos u.
\end{aligned}$$

Notice that we have not written the component of the vector field defining the last (decoupled) equation of system (2.3) as a function of  $u$  alone. For the moment we are not interested to integrate this equation because its present form will help us to obtain the nodal period.

Using the solution of (3.1), the perturbed orbit equation can be written as

$$\begin{aligned}
p_0/r = & 1 + \left[ -\frac{1}{\sqrt{1-x}} \sin u_0 \sin(\sqrt{1-x}(u-u_0)) + \cos(\sqrt{1-x}(u-u_0)) \right] q_0 \\
& + \left[ \frac{1}{\sqrt{1-x}} \cos u_0 \sin(\sqrt{1-x}(u-u_0)) + \sin u_0 \cos(\sqrt{1-x}(u-u_0)) \right] k_0 \\
& + \frac{x}{1-x} [1 - \cos(\sqrt{1-x}(u-u_0))].
\end{aligned}$$

Introducing the quantities  $q_0 = e_0 \cos \omega_0$ ,  $k_0 = e_0 \sin \omega_0$ ,  $v_0 = u_0 - \omega_0$  (which stay for initial conditions) in the above relation we obtain

$$\tilde{p}/\rho = 1 + \tilde{e} \cos \tilde{v}, \quad (3.2)$$



where

$$\begin{aligned}\tilde{p} &= (1-x)p_0, \\ \tilde{e} &= \sqrt{1-(1-x)[1-e_0^2+x(1+e_0\cos v_0)^2]}, \\ \tilde{v} &= \sqrt{1-x}u - \tilde{w}, \\ \tilde{w} &= \sqrt{1-x}u_0 - \arctan \frac{\sqrt{1-x}e_0\sin v_0}{(1-x)e_0\cos v_0 - x}.\end{aligned}$$

The equation (3.2) represents a *precessional* conic section, i.e. an orbit described by a particle moving on a conic section whose focal axis rotates in the plane of the motion. This has been already proved by Newton for the case of the ellipse, as we have stated in our Introduction (see also [4], p. 123 and [16], p. 96).

Notice further that  $\tilde{\omega} = u - \tilde{v}$ , the argument of pericenter of the precessional conic section increases with the increase of  $(1 - \sqrt{1-x})u$ . If the conic section is an ellipse, a first order approximation in  $x$  shows that the pericentre secular shift is  $3\pi\mu/(c^2p_0)$  per revolution, which represents half of the relativistic shift.

Let us see now what kind of precessional conic sections appear in (3.2). Observe first that since  $x$  is always smaller than 1,  $\tilde{e}$  is always real. Denoting by  $\tilde{a} = \tilde{p}/(1 - \tilde{e}^2)$  the semimajor axis of the precessional conic section and using the fact that  $p_0/\rho_0 = 1 + e_0\cos v_0$ , it follows that  $1/\tilde{a} = 1/a_0 + xp_0/\rho_0^2$ . This means that to an unperturbed initial condition of hyperbolic type, i.e. with  $a_0 < -\rho_0/(xp_0)$ , corresponds a precessional ellipse ( $\tilde{a} > 0$ ); if  $a_0 \geq -\rho_0/(xp_0)$ , the orbit is a precessional hyperbola. The expression of  $\tilde{e}$  shows that to an unperturbed initial condition of parabolic type corresponds a precessional ellipse if  $v \in (-\pi, \pi)$ , and a precessional parabola otherwise.

## 4. Nodal Period

The content of this section has applications in astronomy. As we will see below, the precise determination of the nodal period of an orbit is important in observational studies, and Manev's model allows the exact computation of formulas for any value of the initial conditions. We will give below the principles of these computations and provide some of the formulas. Several particular cases can be taken into account, but our intention is not to exhaust them, just to outline the ideas and compute the most significant ones.

From the various types of orbital periods (nodal, quasinodal, anomalistic, etc.) we choose to consider here the *nodal period* defined as

$$T_\Omega = \int_0^{2\pi} \frac{dt}{du} du.$$

There are two reasons that make us prefer the nodal period to any others: it is easily accessible to measurements and allows the study of low eccentric orbits, even of circular ones, which have an unwell defined or a not-at-all defined pericenter.

A perturbative method for the determination of  $T_\Omega$  has been proposed by Zhonglovich, [20], and then extended and generalized by Mioc, [11], [12], [13], to perturbing radial or nonradial forces acting in the orbital plane. These methods provide different orders of approximation for  $T_\Omega$  with respect to a small parameter characterizing the perturbing

factor. Nevertheless, we will not use them here. Instead we will compute an exact formula of the nodal period.

Let us first consider that the unperturbed orbit is an ellipse. From the last equation in (2.3), using (3.2) and the initial conditions (at initial time  $t_0 = 0$ ), we obtain

$$T_\Omega = (\tilde{p}^2/\sqrt{\mu p}) \int_0^{2\pi} [1 + \tilde{e} \cos(\sqrt{1-x}u - \tilde{w})]^{-2} du.$$

Computing further we obtain the exact formula of the nodal period as a function of the initial data:

$$T_\Omega = 2 \left[ \frac{(1-x)p_0}{g_0\mu^{1/3}} \right]^{3/2} \left[ \pi + \arctan \frac{\sqrt{g_0}S_0}{f_0} - \frac{\sqrt{g_0}S_0(f_0 - g_0C_0)}{f_0^2 + g_0S_0^2} \right], \quad (4.1)$$

where

$$\begin{aligned} f_0 &= [(1-x)e_0 \cos v_0 - x] \cos(\sqrt{1-x}(\pi - u_0)) - \sqrt{1-x}e_0 \sin v_0 \sin(\sqrt{1-x}(\pi - u_0)) \\ &\quad + \cos(\pi\sqrt{1-x}), \\ g_0 &= (1-x)[1 - e_0^2 + x(1 + e_0 \cos v_0)^2], \\ S_0 &= \sin(\pi\sqrt{1-x}), \\ C_0 &= \cos(\pi\sqrt{1-x}). \end{aligned}$$

The relation between the perturbed nodal period and the corresponding unperturbed Keplerian period  $T_0 = 2\pi a_0^{3/2}/\sqrt{\mu}$  is

$$T_\Omega = T_0 \left[ \frac{(1-x)(1-e_0^2)}{\pi^{2/3}g_0} \right]^{3/2} \left[ \pi + \arctan \frac{\sqrt{g_0}S_0}{f_0} - \frac{\sqrt{g_0}S_0(f_0 - g_0C_0)}{f_0^2 + g_0S_0^2} \right].$$

Notice that for  $x = 0$ ,  $T_\Omega = T_0$ , so we recover—as expected—the classical Keplerian nodal period.

The formula can be expressed in simpler terms if the initial orbital elements are taken in the ascending node,  $u_0 = 0$ . The nodal period then becomes

$$T_\Omega = 2 \left[ \frac{a_0}{(1+x)\mu^{1/3}} \right]^{3/2} \left[ \pi + \arctan \frac{S_0}{C_0} \sqrt{\frac{1+x}{1-x}} + \frac{x\sqrt{1-x}S_0C_0}{1-x(C_0^2 - S_0^2)} \right].$$

For initial conditions of circular type,  $e_0 = 0$ , the nodal period is given by

$$T_\Omega = 2 \left[ \frac{a_0}{(1+x)\mu^{1/3}} \right]^{3/2} \left( \pi + \arctan \frac{\sqrt{1-x^2}S_0}{f_0} \right) - \frac{\sqrt{1-x^2}S_0[f_0 - (1-x)^2C_0]}{f_0^2 + (1-x^2)S_0^2},$$

where  $f_0 = C_0 - x \cos(\sqrt{1-x}(\pi - u_0))$ .

If the initial conditions are of parabolic type,  $e_0 = 1$ , let us take the initial elements in the ascending node to coincide with the pericentre,  $u_0 = v_0 = 0$ . As we have seen in the previous section, in this case the orbit is of elliptic type, and the nodal period is given by

$$T_\Omega = \frac{1}{4} \left( \frac{p_0}{x\mu^{1/3}} \right)^{3/2} \left[ \pi + \arctan \frac{S_0}{C_0} \sqrt{\frac{x}{1-x}} - \frac{\sqrt{x(1-x)}(1-2x)S_0C_0}{(1-x)C_0^2 + xS_0^2} \right].$$

## 5. The Collision Manifold

We start in this section the qualitative analysis of orbits in the neighborhood of collisions. Since the following results do not depend on the precise values of the constants involved, nor on the system of units, we will simplify things by taking the units such that  $G = 1$ ,  $m_1 = M$  and  $m_2 = M$ . Then the Manev potential is written as  $W = U + V$ , where

$$U(\mathbf{q}) = M/|\mathbf{q}|, \quad V(\mathbf{q}) = \gamma M(M+1)/|\mathbf{q}|^2,$$

and  $\gamma = 3/(2c^2)$ .

The equations of motion (2.3) can be written as a first order system of differential equations

$$\begin{cases} \dot{\mathbf{q}} = \mathbf{p} \\ \dot{\mathbf{p}} = -\nabla W(\mathbf{q}), \end{cases} \quad (5.1)$$

where  $\mathbf{p} = (p_1, p_2) = (M\dot{q}_1, \dot{q}_2)$  is the momentum of the system of particles.

Let  $T(\mathbf{p}) = (M^{-1}p_1^2 + p_2^2)/2$  be the kinetic energy of the system. Then the integral of energy reads

$$T(\mathbf{p}) - W(\mathbf{q}) = h,$$

where  $h$  is the energy constant.

Define the angular momentum function as  $L(\mathbf{q}, \mathbf{p}) = q_1 p_2 - q_2 p_1$ . The integral of the the angular momentum is then given by

$$L(\mathbf{q}, \mathbf{p}) = c,$$

where  $c$  is (from now on) the constant of the angular momentum.

We will further introduce McGehee-type transformations, [10], in order to eliminate the singularity  $\mathbf{q} = (0, 0)$  which occurs in the equations (5.1). Let

$$\begin{cases} q_1 = r \cos \theta \\ q_2 = r \sin \theta \\ p_1 = -x \sin \theta + y \cos \theta \\ p_2 = x \cos \theta + y \sin \theta, \end{cases} \quad (5.2)$$

which is an analytic diffeomorphism. Indeed, notice that the inverse is given by

$$\begin{cases} r = |\mathbf{q}| \\ \theta = \arctan(q_2/q_1) \\ y = \dot{r} = (q_1 p_1 + q_2 p_2)/|\mathbf{q}| \\ x = r\dot{\theta} = (q_1 p_2 - q_2 p_1)/|\mathbf{q}|, \end{cases}$$

and both (5.2) and the inverse are analytic.

The first two equations of the inverse are the standard polar coordinates ( $r > 0, \theta \in [0, 2\pi)$ ), the third is the radial velocity and the fourth represents the tangential velocity.

Using these transformations the equations (5.1) take the form

$$\begin{cases} \dot{r} = y \\ \dot{y} = r^{-1}[x^2 - U(r) - 2V(r)] \\ \dot{\theta} = r^{-1}x \\ \dot{x} = -r^{-1}xy, \end{cases} \quad (5.3)$$

and the energy and angular momentum integrals become

$$\frac{1}{2}(x^2 + y^2) - U(r) - V(r) = h,$$

$$rx = c.$$

Observe that the the four equations in (5.3) are the expressions of the radial velocity, radial acceleration, angular velocity, and tangential acceleration. Notice also that the singularity  $\mathbf{q} = (0, 0)$  is transformed into  $r = 0$ . Our further goal will therefore be to eliminate the variable  $r$  from the denominators of the expressions defining the vector field in (5.3).

Let us further rescale the radial and tangential velocities  $x$  and  $y$ , in order to make one step further in eliminating the singularity from the equations of motion. For this we define the analytic diffeomorphism

$$\begin{cases} v = ry \\ u = rx. \end{cases} \quad (5.4)$$

This will transform the equations (5.3) into the system

$$\begin{cases} \dot{r} = r^{-1}v \\ \dot{v} = x^2 + y^2 - U(r) - 2V(r) \\ \dot{\theta} = r^{-2}u \\ \dot{u} = 0, \end{cases} \quad (5.5)$$

and the energy relation and the angular momentum integral take the form

$$\frac{1}{2}(u^2 + v^2) - rM - \gamma M(M + 1) = r^2h,$$

$$u = c.$$

Let us finally rescale the time using the analytic diffeomorphism

$$d\tau = r^{-2}dt. \quad (5.6)$$

Using also the above energy relation and angular momentum integral, (5.6) will transform the equations (5.5) into the system

$$\begin{cases} r' = rv \\ v' = 2r^2h + rM \\ \theta' = u, \end{cases} \quad (5.7)$$

where  $' = \frac{d}{d\tau}$ . The energy relation and the angular momentum integral are

$$u^2 + v^2 - 2rM - 2\gamma M(M+1) = 2r^2h, \quad (5.8)$$

$$u = c. \quad (5.9)$$

The angular momentum integral shows that, for each solution, there is a constant  $c$ , such that  $u$  and  $\theta'$  take the value of that constant, and consequently  $\theta$  is a linear function of the fictitious time variable  $\tau$ .

Since  $r$  does not further occur in the denominators of the vector field defining the equations (5.7), the singularity has been eliminated, so the system (5.7) is now regularized. Therefore we can extend the equations of motion to the case  $r = 0$ . Indeed, notice that the set

$$\{(r, v, \theta, u) | r = 0\}$$

is invariant for the equations (5.7). Therefore we can extend the phase space to contain this set. Moreover, the energy relation (5.8) also defines an invariant set. We will therefore paste to the phase space the set

$$C = \{(r, v, \theta, u) | u = 0, u^2 + v^2 - 2rM - 2\gamma M(M+1) = 2r^2h\},$$

which is an analytic manifold, and since  $r = 0$  corresponds to collisions, we will call it the *collision manifold*.

The collision manifold was thus obtained by blowing up the collision singularity. Though it has no correspondent in the physical reality, due to the property of continuity of the solutions with respect to the initial data, the study of the flow on the collision manifold will give us information on the behavior of the flow near the collision manifold (i.e. for  $r$  positive and small). From here we can draw conclusions about the behavior of the particles near collision. We will perform this study in the next section.

## 6. The Flow

Let us determine first the shape of the collision manifold. Since  $r = 0$ , the energy relation becomes

$$u^2 + v^2 = 2\gamma M(M+1).$$

In the space of coordinates  $(u, \theta, v)$ , this represents a circular cylinder, and the flow on it is formed by lines parallel with the axis of the cylinder (see Figure 1) if  $u \neq 0$ . For  $u = 0$  we have  $\theta = \text{constant}$ , so the lines  $v = \pm\sqrt{2\gamma M(M+1)}$  on the cylinder are formed by fixed points. Since  $\theta \in [0, 2\pi)$ , by identifying the caps of the cylinder we obtain a 2-dimensional torus. The flow on the torus is given by periodic orbits  $P_v = \{v = k \text{ (const.)}, \theta \in [0, 2\pi)\}$ , (i.e. circles as in Figure 2) for  $v \neq \pm\sqrt{2\gamma M(M+1)}$ , and by a circle formed entirely by fixed points in each of the cases  $v = \pm\sqrt{2\gamma M(M+1)}$ . To reach the collision manifold, and lead—in the physical reality—to a collision between the two particles, an orbit in phase space must tend to one of these periodic orbits or to one of the fixed points.

We will show now that from each fixed point of the circle  $v = \sqrt{2\gamma M(M+1)}$  there ejects one single orbit (see Figure 2), and that to each fixed point of the circle  $v = -\sqrt{2\gamma M(M+1)}$  will tend one single orbit. Indeed, since  $u = 0$  at  $v = \pm\sqrt{2\gamma M(M+1)}$ , it follows from the equations (5.7) that  $\theta = \text{constant}$ , consequently, there will exist an orbit ejecting from every equilibrium of the upper circle, and this orbit is a straight halfline perpendicular on the plane of the circle. The direction of the orbit is away from the equilibrium. Indeed, if  $r$  is sufficiently small (i.e. if the orbit is close enough to the torus),  $v' > 0$ , so  $v$  is increasing. In the same way we prove the second part of the statement.

Let us see now that for every orbit  $P_v$ , with  $0 < v < \sqrt{2\gamma M(M+1)}$  there exists a manifold of orbits, lying on a cylinder, which eject from  $P_v$ . Similarly, for every orbit  $P_v$ , with  $-\sqrt{2\gamma M(M+1)} < v < 0$ , there exists a manifold of orbits, lying on a cylinder, which tend to  $P_v$ . If  $v = 0$ , both types of manifolds exist for  $P_0$ . In order to prove this observe first that since  $u = c$  (constant), all the solutions in the whole phase space lie on concentric circular cylinders having  $Ov$  as symmetry axis. The cylinders intersecting the torus that defines the collision manifold will form the manifolds described in the above statement (see Figure 3). This happens because  $v$  is increasing if  $r$  is sufficiently small, so the orbits constrained to those cylinders, if close enough to the torus, must eject from the periodic orbit if  $0 < v < \sqrt{2\gamma M(M+1)}$  or tend to it if  $-\sqrt{2\gamma M(M+1)} < v < 0$ . The periodic orbit corresponding to  $v = 0$  is the only one which has both types of manifolds: formed by ejecting and collision orbits. Those ejecting lie on the cylinder above the periodic orbit, and those colliding are on the cylinder below it.

The above proof also shows that the orbits lying on cylinders which do not intersect the torus, will not lead to collisions.

Let us look closer now at the collision orbits and understand their physical interpretation. The orbits tending/ejecting to/from equilibria are those colliding such that the curves describing the paths of the particles have a common tangent at the collision instant. In other words, they have zero angular momentum. The orbits tending/ejecting to/from periodic orbits lead to collisions which occur when the particles spiral around each other before colliding. This happens with nonzero angular momentum.

In other words a collision occurs if the particles are close enough together and the angular momentum is sufficiently small, namely  $c \in [-\sqrt{2\gamma M(M+1)}, \sqrt{2\gamma M(M+1)}]$ . The occurrence of this *black hole effect*, as well as the phase space picture, show that the set of initial data leading to collisions has positive measure. This result is already known (see [18]).

Another fact which becomes now obvious from the phase space picture is that the collisions are not *regularizable* with respect to the initial data (see [3], [10]). Mathematically, this means that when tending asymptotically to the torus, the property of continuity of the solutions with respect to the initial data is violated. Indeed, the orbits ejecting from the equilibria, for example, have the trajectory perpendicular to the plane of the circle (see Figure 2), while any orbit ejecting from a periodic orbit (even those infinitely close to the circle of equilibria) eject tangentially from the circle (see Figure 3). Physically, this means that there is no meaningful extension of the solution beyond the collision. Finally observe that in the Newtonian case the rectilinear motion leading to collisions is the limit case of more and more eccentric ellipses, but this is not true for Manev's gravitational law.

## References

- [1] Diacu, F.N.: *The planar isosceles problem for Maneff's gravitational law*, J. Math. Phys. **34** (12) (1993), 5671-5690.
- [2] Diacu, F.N. and Illner R.: *Collision-ejection dynamics for particle systems with quasihomogeneous potentials* (submitted).
- [3] Easton, R.: *Regularization of vector fields by surgery*, J. Differential Equations **10** (1971), 92-99.
- [4] Goldstein, H.: *Classical Mechanics*, Addison-Wesley, Reading MA, 1980.
- [5] Hagihara, Y.: *Celestial Mechanics*, vol. II, part I, The MIT Press, Cambridge, MA, 1975.
- [6] Maneff, G.: *La gravitation et le principe de l'égalité de l'action et de la réaction*, Comptes rendus **178** (1924), 2159-2161.
- [7] Maneff, G.: *Die Gravitation und das Prinzip von Wirkung und Gegenwirkung*, Zeitschrift für Physik **31** (1925), 786-802.
- [8] Maneff, G.: *Le principe de la moindre action et la gravitation*, Comptes rendus **190** (1930), 963-965.
- [9] Maneff, G.: *La gravitation et l'énergie au zéro*, Comptes rendus **190** (1930), 1374-1377.
- [10] McGehee, R.: *Triple collision in the collinear three-body problem*, Inventiones math. **27** (1974), 191-227.
- [11] Mioc, V.: *Extension of a method for nodal period determination in perturbed orbital motion*, Rom. Astron. J. **2** (1992), 53-59.
- [12] Mioc, V.: *A better approximation for period on radially perturbed orbits*, Rev. Anal. Numér. Théor. Approx. **22** (1993), 201-205.
- [13] Mioc, V.: *Nodal period in motion perturbed by a force acting in orbit plane*, Rom. Astron. J. **3** (1993), 73-81.
- [14] Mioc, V.: *Elliptic-type motion in Fock's gravitational field*, Astron. Nachr. **315** (1994), 175-180.
- [15] Mioc, V. and Radu, E.: *Orbits in an anisotropic radiation field*, Astron. Nachr. **313** (1992), 353-357.
- [16] Moulton, F.R.: *An Introduction to Celestial Mechanics*, second edition, Macmillan, London, 1923.
- [17] Poincaré, H.J.: *Sur la stabilité du système solaire*, Annuaire pour l'an 1898 par le Bureau de Longitudes, pp. B. 1-2, Gauthier-Villars, Paris, 1898.
- [18] Saari, D.G.: *Regularization and the artificial earth satellite problem*, Celest. Mech. **9** (1974), 55-72.
- [19] Taratynova, G.P.: *Über die Bewegung von künstlichen Satelliten im nicht-zentralen Schwerefeld der Erde unter Berücksichtigung des Luftwiderstandes*, in Künstliche Erdsatelliten, Reichardt H. and Niekisch E.A. (editors), Akademie Verlag, Berlin, p. 55-64.
- [20] Zhongolovich, I.D.: *Some formulae occurring in the motion of a material point in the attraction field of a rotation level ellipsoid*, Byull. Inst. Teor. Astron. **7** (1960), 521-536 (in Russian).

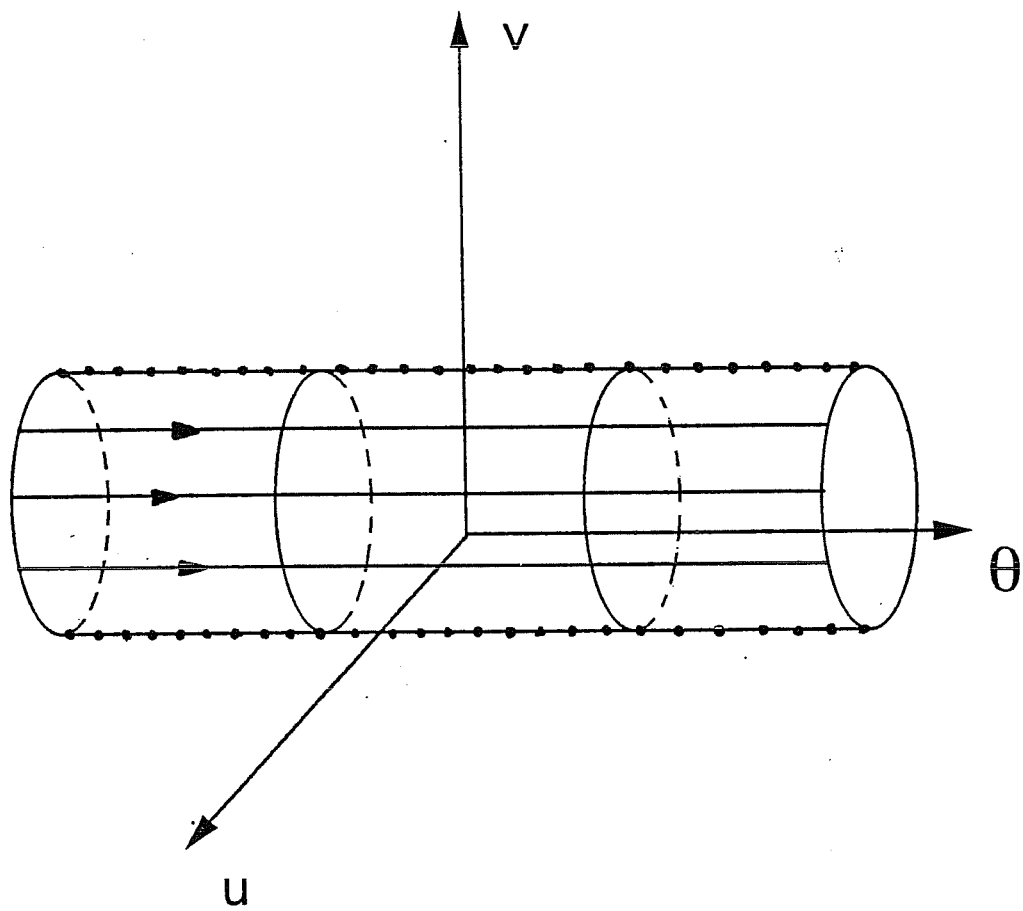


Figure 1.

The collision manifold



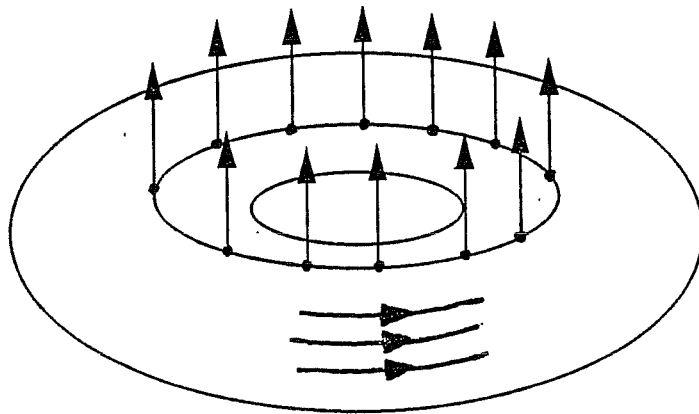


Figure 2

Orbits ejecting from the fixed points

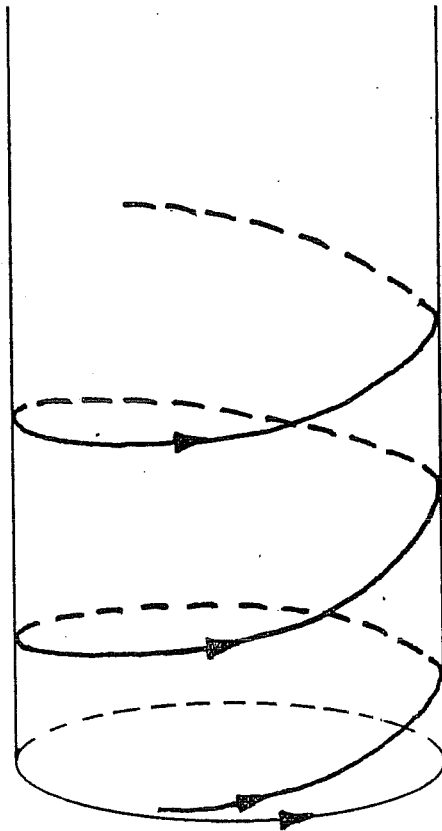


Figure 3

An orbit ejecting from a periodic one